Research Square

Preprints are preliminary reports that have not undergone peer review.
They should not be considered conclusive, used to inform clinical practice,
or referenced by the media as validated information.

A “Three Birds with One Stone” Strategy for the Pretreatment of Swine Wastewater Using Modified Attapulgite: Purification Mechanisms of Crystallization–Coagulation–Adsorption

Fanshuo Zeng
Tianjin University of Science & Technology
Jingshuang Yan
Tianjin University of Science & Technology
Linlin Hao
xilan.2009@tust.edu.cn

Tianjin University of Science & Technology

Research Article

Keywords: Attapulgite, Swine wastewater, Coagulation, Struvite crystallization, Synergistic purification

Posted Date: November 4th, 2026

DOI: https://doi.org/10.21203/rs.3.rs-11346677/v1

License: This work is licensed under a Creative Commons Attribution 4.0 International License.
Read Full License

Additional Declarations: No competing interests reported.

Abstract

This study developed a novel attapulgite-based coagulant (ATPC) to address the high turbidity, high organic content, and high NH_4^+ concentration of swine wastewater. ATPC was synthesized from natural attapulgite (palygorskite) (ATP) through a synergistic modification strategy that combined high-temperature calcination, sulfuric acid leaching, and alkali-induced polymerization. The optimal preparation conditions were determined as follows: calcination temperature of 600°C, sulfuric acid concentration of 25%, solid–liquid ratio of 1:5, and polymerization pH of 3. Under these conditions, ATPC achieved a turbidity removal efficiency of 98.8% for swine wastewater. Compared with conventional polyaluminum chloride (PAC), ATPC formed denser flocs that settled considerably faster. Coupling ATPC with magnesium salts induced struvite crystallization and increased the NH_4^+ removal efficiency from less than 10% to approximately 50%. At the optimal aging time of 12 h, the functional component accounted for 48.8% of $[Fe(III) + Al(III)]_T$. The zeta potential trend indicates that charge neutralization is the primary mechanism of ATPC, in which high-valent cations are essential for destabilizing colloids, while the insoluble particles strengthen the floc structure and promote sedimentation through bridging effects. The as-prepared ATPC is an eco-friendly natural mineral coagulant with promising prospects for the advanced treatment of swine wastewater.

1. Introduction

China is the world's largest pork producer, with an intensive pig farming industry. China accounts for more than 50% of global pork production (J. Wang et al., 2025), and its pork output reached a record 59.4 million tons in 2025, corresponding to an annual slaughter volume of approximately 720 million head. The pollution caused by the discharge of large amounts of pig manure and wastewater has become a major constraint on the sustainable development of the pig farming industry.

Swine wastewater is characterized by three typical features: a high turbidity, a high chemical oxygen demand (COD), and a high NH_4^+ content (Ando et al., 2025; Deng et al., 2023). Most of the organic pollutants in swine wastewater are present as suspended solids (SS), therefore, effective solid–liquid separation before biological treatment is essential to reduce the SS concentration (C. Wang et al., 2025). Coagulation–sedimentation is a key pretreatment unit for swine wastewater, yet conventional coagulants such as PAC form loose flocs, settle slowly, and remove NH_4^+ poorly (Jia & Wang, 2023). Developing efficient, low-cost, and eco-friendly coagulants capable of removing multiple pollutants is therefore of considerable practical importance.

A wide range of coagulants has been investigated for swine wastewater treatment. The addition of aluminum salts, iron salts, or polymeric flocculants such as polyacrylamide (PAM) destabilizes fine suspended particles and colloids and promotes their aggregation into large flocs that can be removed by sedimentation (Tijjani Usman et al., 2023; Zhao, Y. et al., 2023), thereby markedly reducing COD, turbidity, and part of NH_4^+ (Waras et al., 2024). Liu et al. (2022) achieved sulfate and nitrate removal rates of

99.3% and 99.9%, respectively, by adding heat-treated PAC, providing a route for treating flue gas desulfurization wastewater without generating secondary waste. Du et al. (2024) used a shell algae-based magnetic coagulant to remove high-concentration emulsified oil from wastewater, with the assistance of PAM, achieved turbidity and COD removal rates of 95.7% and 71.6%, respectively, together with excellent recyclability. Chen et al. (2024) studied the removal of polyethylene microplastics using laminarin combined with PAC and obtained a maximum removal efficiency of 91.5%.

ATP is a magnesium-rich aluminosilicate clay with a characteristic chain-layer structure. Because of its large specific surface area and good adsorption capacity, ATP has attracted considerable interest in water treatment (Gianni et al., 2021; Marmolejo-Contreras et al., 2025; J. Yang et al., 2021). Natural ATP, however, contains impurities and suffers from pore blockage, which limits its performance in direct application (Gong et al., 2021; Shi, T. et al., 2022). Common modification methods include calcination, acid leaching, and alkali treatment (Chen et al., 2023). Acid leaching effectively dissolves pore impurities and thus increases the specific surface area and the number of active sites; calcination removes structural water and activates mineral surfaces; and alkali treatment induces leached metal ions to form hydroxyl polymers with high coagulation activity. Hussein et al. (2025) modified ATP with hydrochloric and acetic acids for copper removal and obtained an adsorbent with a maximum adsorption capacity of 277.2 mg/g. Yan et al. (2023) prepared quaternized ATP for the removal of acetone and phenol from wastewater and achieved removal efficiencies of approximately 65.7% and 78.7%, respectively, under optimized conditions. K. Yang et al. (2023) used MgO-modified ATP/biochar composites to remove Cd(II) and reached a maximum adsorption capacity of 441.1 mg/g, which is 4.6 times that of the raw material. Although modified ATP has been widely studied for water treatment, its systematic application to livestock wastewater remains limited and requires further theoretical and practical investigation.

This study proposes a synergistic modification strategy—high-temperature calcination–sulfuric acid leaching–alkali-induced polymerization—to prepare a novel ATP-based coagulant. The objectives are to systematically optimize the preparation conditions of ATPC, to characterize its structural properties by complementary techniques, and to elucidate the synergistic crystallization–coagulation–adsorption mechanism operating during swine wastewater treatment. Coupling with magnesium salts induces struvite crystallization, which enhances ammonia nitrogen removal. This work is intended to provide a new technical approach and a theoretical basis for the efficient and low-cost pretreatment of swine wastewater.

2. Materials and Methods

2.1 Experimental Materials and Reagents

Raw attapulgite (purity > 90%) was obtained from Xuyi, Jiangsu Province, China. Swine wastewater was collected from a large-scale pig farm and had the following characteristics: pH 8.1 ± 0.3, turbidity 300 ± 10 NTU, COD 4791 ± 100 mg/L, NH_4^+ 880 ± 10 mg/L, and TP 113 ± 5 mg/L. The main reagents were

sulfuric acid (H_2SO_4, AR), sodium hydroxide (NaOH, AR), magnesium chloride ($MgCl_2$, AR), potassium dihydrogen phosphate (KH_2PO_4, AR), PAC (98%), and PAM.

2.2 Preparation of ATPC

ATPC was prepared by a calcination–acid leaching–alkali polymerization process. Raw ATP was placed in a muffle furnace and calcined at 600 ℃ for 2 h at a heating rate of 15 ℃/min. The calcined product was mixed with 25% sulfuric acid at a solid–liquid ratio of 1:5 and leached in a high-pressure reactor at 60 ℃ for 8 h (Bakalár et al., 2025). The mixture was then slowly adjusted to pH 3 with 1 mol/L NaOH and aged for 12 h (Hao et al., 2025). The resulting product was dried at 105 ℃, ground, and sieved to obtain ATPC powder.

2.3 Characterization Methods

X-ray diffraction (XRD, Bruker D8 Advance) was used for phase analysis, and scanning electron microscopy (SEM, SU-1510) was used to observe the surface morphology. Fourier-transform infrared spectroscopy (FT-IR, Bruker Vertex 70) was used to identify functional groups, and X-ray fluorescence spectrometry (XRF, XRF-1800) was used for elemental composition analysis. The specific surface area was measured with a surface area analyzer (BET, Autosorb-iQ), and the zeta potential was determined with a zeta potential analyzer (Zetasizer Nano ZS90).

2.4 Coagulation Experiments

Coagulation tests were conducted in a six-paddle jar tester. A 200 mL wastewater sample was placed in a beaker, a predetermined amount of ATPC was added, and the mixture was stirred rapidly at 250 r/min for 3 min and then slowly at 50 r/min for 15 min. After 30 min of settling, the supernatant was sampled 2 cm below the liquid surface and analyzed for turbidity, COD, NH_4^+–N, total nitrogen (TN), TP, and other parameters. The removal efficiency (R, %) of each pollutant was calculated as $R = (C_0 - C)/C_0 \times 100\%$, where C_0 and C are the pollutant concentrations in the raw wastewater and in the supernatant after treatment, respectively. All coagulation experiments were performed in triplicate.

To enhance ammonia nitrogen removal, struvite crystallization was coupled with the coagulation process. ATPC, KH_2PO_4 (to adjust the N:P molar ratio to approximately 1:1), and $MgCl_2$ were added to the wastewater, the pH was adjusted to 9, and the coagulation experiments were carried out as described above.

3. Results and Discussion

3.1 Optimization of ATPC Preparation Conditions

Single-factor experiments were conducted to examine the effects of the calcination temperature, sulfuric acid concentration, acid leaching solid–liquid ratio, and polymerization pH on the turbidity and COD removal efficiencies of swine wastewater treated with ATPC.

As shown in Fig. 1a, the calcination temperature markedly affected the coagulation performance of ATPC. At a calcination temperature of 600°C, ATPC showed the best coagulation performance, with a residual turbidity of 26.4 NTU and a turbidity removal efficiency of 93.4%, accompanied by a COD removal efficiency of 35.4%. When the calcination temperature was increased to 700°C, the coagulation performance decreased only slightly, whereas the COD removal efficiency was clearly lower. A further increase to 800°C raised the residual turbidity to 41.9 NTU and lowered the COD removal efficiency to 11.2%. A moderate calcination temperature removes water molecules in different states from the ATP crystal structure, which reduces their occupation of the active sites on the ATP surface and promotes the formation of new, more active Si–OH and Mg–OH hydroxyl groups. At 800°C, however, chemical bonds such as Si–O–Si and Al–O within the crystal break, and the fibrous crystal structure gradually collapses and agglomerates, transforming into an amorphous or glassy phase (Liu, P. et al., 2025). This transformation accounts for the decreases in both turbidity and COD removal. A calcination temperature of 600°C was therefore selected as the optimum.

As shown in Fig. 1b, both turbidity and COD concentration continuously declined as the sulfuric acid concentration increased from 15% to 25%, reaching their minimum values at 25%, at which the residual turbidity was 18.3 NTU and the COD concentration was 1025 mg/L. When the acid concentration exceeded 25%, however, both the turbidity and the COD concentration began to increase. In the low-to-moderate concentration range, an increase in the acid concentration released more Mg^{2+} and Al^{3+} ions from the framework by ion exchange, which resulted in more extensive protonation of the material surface and increased the positive surface charge of ATPC, thereby enhancing charge neutralization. When the acid concentration exceeded 25%, in contrast, the excessive H^{+} attacked and dissolved the host lattice that maintains the ATP nanofiber structure, which compromised the integrity of the Si–Mg–Al framework and in turn weakened the physical adsorption capacity of the material. Therefore, considering both the retention of the pore structure and the enhancement of the surface charge, a sulfuric acid concentration of 25% was selected as the optimum for acid leaching.

Figure 1c shows that, over the solid–liquid ratio range from 1:1 to 1:5, the turbidity of the supernatant decreased from approximately 29.3 to 15.1 NTU and the COD concentration decreased from approximately 1207 to 982 mg/L as the acid dosage increased, indicating that the coagulation performance improved continuously and reached its optimum at a solid–liquid ratio of 1:5. When the solid–liquid ratio was further decreased to 1:6, the turbidity remained almost unchanged, whereas the COD removal deteriorated and the COD concentration rose again to approximately 1099 mg/L. Therefore, a solid–liquid ratio of 1:5 was selected as the optimum for acid leaching.

The polymerization pH determines the hydrolysis–polymerization species of the leached metal ions (Al^{3+}, Fe^{3+}) and thus the charge neutralization capacity of the coagulant. As shown in Fig. 1d, as the pH increased from 1 to 4, the coagulation performance of ATPC first improved markedly and then decreased slightly, with the optimum at pH 3 (residual turbidity 22.1 NTU; removal efficiency 92.9%). Under strongly acidic conditions (pH 1), the leached Al^{3+} and Fe^{3+} exist mainly as soluble mononuclear hydroxyl complexes with weak charge neutralization, which results in poor coagulation. As the pH increases, the

proportion of Fe^{3+} and Al^{3+} that hydrolyze to form polynuclear hydroxyl complexes increases; these complexes carry a high positive charge and effectively attract the negatively charged colloids in water, destabilizing and aggregating them through charge neutralization. At pH 4, Fe^{3+} and Al^{3+} rapidly combine with OH^- to form non-polymerizable hydroxides such as $Al(OH)_3$ and $Fe(OH)_3$, which weakens charge neutralization and reduces the turbidity removal efficiency (Dhrubo et al., 2023). A polymerization pH of 3 was therefore selected as the optimum.

3.2 Characterization of ATP and ATPC

XRD analysis (Fig. 2a) showed that raw ATP contained impurities such as quartz (2θ = 26.7°) and calcium carbonate. After modification, the intensity of the quartz peak decreased, the calcium carbonate peak disappeared completely, and a calcium sulfate peak appeared, which indicates that sulfuric acid modification converted calcium carbonate into calcium sulfate and thus altered the mineral composition and surface properties of ATP (Tsou et al., 2023). The FT-IR spectra (Fig. 2b) showed that the hydroxyl peaks associated with Mg^{2+} in raw ATP (3697.7 and 3623.4 cm^{-1}) disappeared after modification, indicating that the acid treatment dissolved octahedrally coordinated cations and destroyed the original hydroxyl structure. In addition, the carbonate peak at 1438.2 cm^{-1} disappeared, and a new peak appeared at 1141.7 cm^{-1}, which is attributed to the introduction of SO_4^{2-} or to the recombination of leached metal ions with the silicate framework.

BET analysis (Fig. 2c, d) indicated that the N_2 adsorption–desorption isotherm of raw ATP was type IV with an H3 hysteresis loop, suggesting the presence of slit-shaped mesopores (Nouj et al., 2026). After modification, the adsorption and desorption branches of ATPC almost overlapped, the mesoporous structure disappeared, the specific surface area decreased markedly from 49.4 to 6.9 m^2/g, and the pore volume decreased from 0.067 to 0.011 cm^3/g. This is because the acid-dissolved products filled the original pores, and these dissolved products are the key components responsible for coagulation. XRF analysis (Table 1) showed that, after modification, the Si content decreased dramatically (46.6% → 4.3%), indicating disruption of the silica–oxygen tetrahedral network; the Ca content decreased substantially (15.73% → 0.54%), confirming carbonate dissolution; the S content increased sharply (0.08% → 55.1%) owing to the sulfate introduced during acid leaching; and the Al content increased (17.14% → 26.54%), suggesting conversion of Al from aluminosilicate forms into aluminum sulfate and aluminum polymers.

Table 1
Elemental composition of ATP and ATPC

ATP	Na	Mg	Al	Si	S	Cl	K	Ca	Fe
	1.24	**1.99**	**17.14**	**46.6**	**0.08**	**0.07**	**3.16**	**15.73**	**12.32**
ATPC	1.63	2.98	26.54	4.30	55.10	6.26	0.84	0.54	1.82

Figure 3 clearly shows that raw ATP has an intact lamellar structure in which the sheets are closely stacked and have distinct boundaries. This dense lamellar arrangement gives raw ATP a relatively

smooth surface, and its specific surface area originates mainly from the interlayer spaces. After modification, ATPC shows a different micromorphology: the sheets are exfoliated, and the resulting fine crystal fragments readily agglomerate, because of their imbalanced surface charge, to form an agglomerated structure. Elemental mapping provides an intuitive means of examining the spatial distribution, uniformity, and enrichment patterns of the elements in ATP and ATPC, and the distributions of selected elements are shown in Fig. 4. After modification, Al in ATPC still shows a uniform distribution similar to that in ATP, with no obvious local enrichment or depletion. The pronounced increase in S after modification is mainly due to the sulfate introduced, which is loaded on the material surface. The Fe signal appeared weaker, which can be attributed partly to the substantial increase in S and partly to the fact that a small amount of Fe became more uniformly distributed on the surface after acid leaching modification.

3.3 Effect of ATPC on Turbidity Removal from Swine Wastewater

3.3.1 Effect of ATPC Dosage

Figure 5a shows that the turbidity removal efficiency first decreased and then increased as the ATPC dosage increased. At dosages of 3500–4500 mg/L, the removal efficiency exceeded 98%. The best performance was obtained at 4500 mg/L, with a residual turbidity of 5.38 NTU and a removal efficiency of 98.8%, whereas a further increase in dosage decreased the removal efficiency to 96.9%. This is because an excess of coagulant causes charge reversal on the colloids and thus enhances electrostatic repulsion (Zhu et al., 2025).

3.3.2 Effect of Initial pH

With the ATPC dosage fixed at 3500 mg/L, the pH was adjusted from 2 to 9. Figure 5b shows that the turbidity removal efficiency first increased and then decreased as the pH increased. Under strongly acidic conditions (pH < 4), coagulation was poor, mainly because Fe^{3+} and Al^{3+} hydrolyze insufficiently. Under weakly alkaline conditions (pH 9), coagulation was optimal, with a turbidity removal efficiency of 98.84%, because alkaline conditions promote the hydrolysis and polymerization of Fe^{3+} and Al^{3+} and thereby generate polynuclear, high-valent cations that effectively adsorb the negatively charged colloids. At pH > 9, the turbidity increased again, as excess OH^- reacts with Al/Fe ions to form hydroxide precipitates that interfere with coagulation (Y. Wang et al., 2026). ATPC therefore has a wide applicable pH range (removal efficiency > 92% at pH 4–10), with an optimum at pH 9.

3.4 Effect of ATPC on Ammonia Nitrogen Removal from Swine Wastewater

ATPC alone gave only a limited NH_4^+ removal efficiency (< 12%), because NH_4^+ is a stable soluble cation that is difficult to remove directly by coagulation-sedimentation. To overcome this limitation, struvite crystallization was adopted (Xia et al., 2025). The struvite crystallization reaction is as follows:

$Mg^{2+} + NH_4^+ + PO_4^{3-} + 6H_2O \rightarrow MgNH_4PO_4 \cdot 6H_2O \downarrow$ (1)

The molar ratio of Mg^{2+}:NH_4^+:PO_4^{3-} is the key factor in struvite crystallization, and the theoretical optimum for maximum NH_4^+ and P removal is 1.2:1:1. Because the phosphorus concentration in the swine wastewater was only 113 mg/L, additional KH_2PO_4 was required to adjust the N:P molar ratio to approximately 1:1. Moreover, since the magnesium content of ATPC was only 2%, an external magnesium source was also needed. In the treatment of real wastewater with an ATPC dosage of 3500 mg/L, a supplemented phosphorus source, and 3000 mg/L $MgCl_2$ at pH 9, the NH_4^+ removal efficiency increased from less than 10% to approximately 50% (Fig. 6a).

As shown in Fig. 6b, the NH_4^+ concentration decreased gradually as the pH increased from 6 to 9, and the removal efficiency reached a maximum at pH 9, at which the NH_4^+ removal efficiency was 50%. When the pH was increased to 10, the NH_4^+ concentration rose slightly and the removal efficiency decreased marginally. The solubility product (K_{sp}) of struvite is lowest at pH 8–9, where struvite is most stable, which promotes more efficient removal of NH_4^+ by precipitation. When the pH exceeds 9, an excessively high pH may change the speciation of the phosphate ions and thereby initiate a series of side reactions, as shown in Eqs. (2) and (3). The optimum pH of the swine wastewater was therefore 9.

(2)

(3)

3.5 Coagulation Performance Comparison: ATPC vs. PAC

Figure 7a shows that the removal efficiencies of turbidity and COD for both ATPC and PAC increased with dosage, and that ATPC performed slightly better in COD and NH_4^+ removal. ATPC, however, showed clear advantages in settling speed and floc compactness: compared with PAC, it formed denser flocs that settled much faster. The floc volume of ATPC decreased to approximately 10% within 5 min, whereas that of PAC remained at 40% even after 30 min (Fig. 7b). This is because attapulgite has a rod-like crystal structure that acts as a natural backbone, forming a dense three-dimensional floc network with low porosity and strong binding. The superior settleability of ATPC can therefore considerably reduce the hydraulic retention time (HRT) required in sedimentation tanks and thereby improve operational efficiency in practical applications.

3.6 Speciation Analysis of Aluminum–Iron Polymers in ATPC

The Ferron timed complexation colorimetric method was used to analyze the speciation of the Al–Fe polymers in ATPC prepared with different aging times (Yuan et al., 2025). According to their reaction rates with the Ferron reagent, the Al–Fe polymers were classified into three categories: the immediately reactive species $[Fe(III) + Al(III)]_a$ (mononuclear hydroxyl complexes and oligomers), the species reactive within a certain time $[Fe(III) + Al(III)]_b$ (polynuclear hydroxyl complexes and medium polymers, i.e., the effective components), and the non-reactive species $[Fe(III) + Al(III)]_c$ (high polymers). A standard curve

was constructed, the absorbance was measured at different time points, and the distribution of each species was calculated in combination with the total Al/Fe content determined by ICP-MS. As shown in Fig. 8a, with increasing aging time the content of $[Fe(III) + Al(III)]_a$ first increased and then decreased, the content of $[Fe(III) + Al(III)]_b$ also increased initially and then decreased, and the content of $[Fe(III) + Al(III)]_c$ changed accordingly. During aging for 4–12 h, the hydrolyzed $[Fe(III) + Al(III)]_a$ (oligomers) gradually polymerized through hydroxyl bridging to form $[Fe(III) + Al(III)]_b$ (medium polymers) of moderate molecular weight. Because the formation rates of $[Fe(III) + Al(III)]_a$ and $[Fe(III) + Al(III)]_b$ were higher than that of $[Fe(III) + Al(III)]_c$ during this period, the proportion of high polymers decreased gradually. At an aging time of 12 h, the content of $[Fe(III) + Al(III)]_b$ reached a maximum and accounted for 48.82% of the total $[Fe(III) + Al(III)]_T$. Since $[Fe(III) + Al(III)]_b$ is the most effective component, a higher content of it corresponds to better coagulation performance. The optimal aging time was therefore 12 h, at which ATPC contains the highest proportion of active medium polymers and exhibits the best coagulation performance.

Colloidal particles in swine wastewater carry surface charges, and the resulting electrostatic repulsion stabilizes them in water and hinders their aggregation and settling. Changes in the zeta potential directly reflect the charge neutralization capacity of a coagulant, which is a key factor governing coagulation efficiency (Niu et al., 2023). The zeta potentials of water samples treated with different coagulant dosages are shown in Fig. 8b. Without coagulation, the zeta potential was approximately − 30 mV, indicating strongly negatively charged colloidal surfaces. As the coagulant dosage increased, the zeta potential increased, indicating that cations released from ATPC effectively neutralized part of the negative charges, which reduced colloid stability and led to destabilization and aggregation. When the zeta potential approached 0 mV, the electrostatic repulsion between colloids was essentially eliminated; this represents the optimal coagulation condition, in which van der Waals forces dominate and favor the formation of large, dense flocs. The zeta potential trend confirms that the primary mechanism of ATPC is charge neutralization. High-valent cations dissociated from the soluble salts are essential for charge neutralization and colloid destabilization, whereas the insoluble particles strengthen the floc structure and promote sedimentation through bridging effects.

3.7 Synergistic Coagulation Effect of Soluble Salts and Insoluble Particles in ATPC

The insoluble particles and soluble salts in ATPC were separated, dried, ground, and then used individually in coagulation experiments under identical conditions. Figure 9 shows pronounced differences in the residual COD concentrations of the supernatant after treatment with ATPC, the isolated insoluble particles, and the isolated soluble salts. As the dosage increased from 1000 to 5000 mg/L, the residual COD decreased for all three materials, but their coagulation performances differed markedly. ATPC performed best, giving a residual COD concentration of 1153.21 mg/L at a dosage of 5 g/L, which corresponds to a removal efficiency of 75.9%. In contrast, the isolated insoluble particles alone achieved only 21.8% COD removal at the same dosage, and the isolated soluble salts alone

achieved only 7.6%. The insoluble particles mainly retain the silicate–magnesium–aluminate framework of ATP and therefore possess some physical adsorption capacity and a gravity-settling effect; however, because they lack the ability to regulate surface charge, their capacity to capture dissolved organic matter and small colloids is weak, and their removal is therefore mainly physical. The isolated soluble salts alone can only achieve limited colloid destabilization by double-layer compression and have almost no capacity to remove macromolecular dissolved pollutants. These results demonstrate that ATPC is an efficient and stable coagulant material whose excellent performance arises from the synergistic interaction between the solid framework and the active sites generated on the surface by modification. The removal of COD from swine wastewater by ATPC therefore involves not only physical adsorption but also the encapsulation of organic matter during the sedimentation of the flocs formed during coagulation, which achieves a synergy between adsorption and coagulation.

Conclusion

A novel attapulgite-based coagulant (ATPC) was successfully prepared by a synergistic high-temperature calcination–sulfuric acid leaching–alkali-induced polymerization method. The optimal preparation conditions were a calcination temperature of 600°C, a sulfuric acid concentration of 25%, a solid–liquid ratio of 1:5, a polymerization pH of 3, and an aging time of 12 h. ATPC exhibited excellent coagulation performance for swine wastewater, and at the optimal dosage the turbidity removal efficiency exceeded 98% for real wastewater. The core mechanism lies in the synergy between charge neutralization by the soluble salts and adsorption bridging/netting by the insoluble particles, which produces dense, fast-settling flocs that outperform those of conventional PAC. Coupling with magnesium salts to induce struvite crystallization effectively overcame the poor NH_4^+ removal of ATPC alone, and under optimized conditions the NH_4^+ removal efficiency increased from less than 10% to approximately 50%. The resulting ATPC-based enhanced primary coagulation pretreatment process showed a pronounced treatment effect on real swine wastewater, with final effluent COD and NH_4^+ concentrations of 1153.2 mg/L and 443.8 mg/L, respectively. The as-prepared ATPC is an eco-friendly, high-performance inorganic mineral coagulant with promising prospects for the treatment of swine wastewater and other high-strength organic wastewaters.

Declarations

Funding

This study is funded by Tianjin University of Science and Technology. (Grant No. 2400050045).

Author Contribution

Fanshuo Zeng: Writing – original draft, Validation, Methodology, Conceptualization; Jingshuang Yan: Visualization, Methodology, Investigation, Data curation, Formal analysis. Linlin Hao: Writing – review &

editing, Visualization, Methodology, Formal analysis, Resources, Funding acquisition.

Acknowledgement

The authors thank the anonymous reviewers for their valuable suggestions to improve the quality of this manuscript.

Data Availability

Data AvailabilityAll data generated or analyzed during this study are included in this published article and its supplementary information files.

References

1. Ando, T., Ananda, R. U., Ryo, N., & Harmayani, K. D. (2025). Pig farm manure pollution and water quality management in tropical islands: Case studies of Okinawa Main Island and Bali Island. *International Journal of River Basin Management*. 1–11. https://doi.org/10.1080/15715124.2025.2544623
2. Bakalár, T., Pavolová, H., Hajduová, Z., Thomas, M., Bednárová, L., & Hromják, M. (2025). Statistical analysis of acid treatment of different types of clay minerals. *Acta Montanistica Slovaca*, *30*(3), 661–670. https://doi.org/10.46544/ams.v30i3.08
3. Chen, J., Lin, J., Li, W., Wang, Y., & Huang, H. (2024). Coagulative removal of polyethylene microplastics using polyaluminum chloride in conjunction with laminarin. *Chemical Engineering Research and Design*, *212*, 230–239. https://doi.org/10.1016/j.cherd.2024.11.015
4. Chen, J., Lu, X., Wang, D., Xiu, P., & Gu, X. (2023). Effective depolymerization of alkali lignin using an attapulgite-$Ce_{0.75}Zr_{0.25}O_2$(ATP-CZO)-supported cobalt catalyst in ethanol/isopropanol media. *Chinese Journal of Chemical Engineering*, *57*(5), 50–62. https://doi.org/10.1016/j.cjche.2022.08.018
5. Deng, L., Zheng, D., Zhang, J., Yang, H., Wang, L., Wang, W., He, T., & Zhang, Y. (2023). Treatment and utilization of swine wastewater – A review on technologies in full-scale application. *Science of the Total Environment*, *880*, Article 163223. https://doi.org/10.1016/j.scitotenv.2023.163223
6. Dhrubo, A. A. K., Jannat, M., & Hossain, M. S. (2023). Enhancing the performance of coagulants for wastewater treatment by varying and optimizing the experimental parameters. *Journal of Water Process Engineering*, *55*, Article 104144. https://doi.org/10.1016/j.jwpe.2023.104144
7. Du, S., Liu, C., Cheng, P., & Liang, W. (2024). Chitosan-based grafted cationic magnetic material to remove emulsified oil from wastewater: Performance and mechanism. *Processes*, *12*(4), Article 797. https://doi.org/10.3390/pr12040797
8. Gianni, E., Lazaratou, C. V., Panagopoulos, G., Sarantari, P., Martsouka, F., Papagiannopoulos, K., Panagiotaras, D., & Papoulis, D. (2021). Raw and modified palygorskite in water treatment

applications for low-concentration ammonium removal. *Water Environment Research*, *93*(10), 1979–1994. https://doi.org/10.1002/wer.1570

9. Gong, X., Zhang, Z., & Wang, H. (2021). Effects of *Gleditsia sinensis* pod powder, coconut shell biochar and rice husk biochar as additives on bacterial communities and compost quality during vermicomposting of pig manure and wheat straw. *Journal of Environmental Management*, *295*, Article 113136. https://doi.org/10.1016/j.jenvman.2021.113136
10. Hao, L., Yan, J., Guo, J., Wang, N., & Zeng, M. (2025). Convert iron tailings waste into a novel Mg-Fe-Al hybrid magnetic coagulant for enhanced pretreatment of swine wastewater. *Journal of Environmental Chemical Engineering*, *13*(2), Article 115546. https://doi.org/10.1016/j.jece.2025.115546
11. Hussein, A. F., Al-Bidry, M. A., & Wasiti, A. A. A. (2025). Investigation and evaluation of palygorskite microstructure following acid pretreatment and its potential use as an adsorbent for copper. *Scientific Reports*, *15*(1), Article 3813. https://doi.org/10.1038/s41598-025-88449-8
12. Jia, R., & Wang, W. (2023). Performance of chitosan/PAC enhanced coagulation for low-temperature and low-turbidity Pi River source water. *Desalination and Water Treatment*, *306*, 199–207. https://doi.org/10.5004/dwt.2023.29842
13. Liu, J., Wang, Y., Wang, Y., Wang, Z., Wang, X., Kong, F., Yan, Z., Li, T., & Wang, L. (2022). High performance of commercial PAC on the simultaneous desulfurization and denitrification of wastewater from a coal-fired heating plant. *Frontiers in Chemistry*, *10*, Article 916368. https://doi.org/10.3389/fchem.2022.916368
14. Liu, P., Wang, X., & Zhang, W. (2025). The development of an efficient precipitation-flotation-dewatering (PFD) process for acid mine drainage treatment. *Separation and Purification Technology*, *353*, Article 128542. https://doi.org/10.1016/j.seppur.2024.128542
15. Marmolejo-Contreras, J. C., Leyva-Ramos, R., Carrales-Alvarado, D. H., Valdez-García, G. D., & Naranjo-Zapot, B. V. (2025). Adsorption of ammonium from water solution onto natural and modified palygorskite. *MRS Advances*, *10*(3), 301–307. https://doi.org/10.1557/s43580-024-01027-4
16. Niu, Z., Su, Y., Li, J., An, F., & Liu, T. (2023). Effect of attapulgite application on aggregate formation and carbon and nitrogen content in sandy soil. *Sustainability*, *15*(16), Article 12511. https://doi.org/10.3390/su151612511
17. Nouj, N., Abelouah, M. R., Idbella, M., Hamou, A. B., Chaoui, A., Hafid, N., & Alem, N. E. (2026). Unlocking the full potential of agro-waste bio-coagulants for industrial wastewater treatment using pH-first optimization. *Water, Air, & Soil Pollution*, *237*(2), Article 97. https://doi.org/10.1007/s11270-025-08729-x
18. Shi, T., Liu, Y., Zhang, Y., Lan, Y., Zhao, Q., Zhao, Y., & Wang, H. (2022). Calcined attapulgite clay as supplementary cementing material: Thermal treatment, hydration activity and mechanical properties. *International Journal of Concrete Structures and Materials*, *16*(1), Article 10. https://doi.org/10.1186/s40069-022-00499-8

19. Tijjani Usman, I. M., Ho, Y.-C., Baloo, L., Lam, M.-K., Show, P.-L., & Sujarwo, W. (2023). Comprehensive review of modification, optimisation, and characterisation methods applied to plant-based natural coagulants (PBNCs) for water and wastewater treatment. *Sustainability*, *15*(5), Article 4484. https://doi.org/10.3390/su15054484
20. Tsou, C.-H., Shui, Y.-J., Du, J., Yao, W.-H., Wu, C.-S., Suen, M.-C., & Chen, S. (2023). Characterization and morphology of nanocomposite hydrogels with a 3D network structure prepared using attapulgite-enhanced polyvinyl alcohol. *Polymers*, *15*(11), Article 2535. https://doi.org/10.3390/polym15112535
21. Wang, C., Wang, H., Zheng, R., Liu, D., Zhang, Q., Lu, H., Wang, X., & Liu, D. (2025). Piggery wastewater treatment by microalgae: Mechanisms and technologies. *Algal Research*, *91*, Article 104205. https://doi.org/10.1016/j.algal.2025.104205
22. Wang, J., Zhao, C., & Chen, S. (2025). Analysis of convergence trends and driving factors of environmental efficiency of pig farming in China. *Frontiers in Sustainable Food Systems*, *9*, Article 1467378. https://doi.org/10.3389/fsufs.2025.1467378
23. Wang, Y., Yang, X., Wu, X., Pan, Y., Yang, Z., Xie, F., & Zhu, G. (2026). Evaluation of polymeric silico-aluminum-ferric coagulant (PSAC) derived from volcanic rock in removal of algae and phosphorus from water. *Processes*, *14*(7), Article 1121. https://doi.org/10.3390/pr14071121
24. Waras, M. N., Zabidi, M. A., Ismail, Z., Sangaralingam, M., Gazzali, A. M., Harun, M. S. R., Aziz, M. Y., Mohamed, R., & Najib, M. N. M. (2024). Comparative analysis of water quality index and river classification in Kereh River, Penang, Malaysia: Impact of untreated swine wastewater from Kampung Selamat pig farms. *Water Environment Research*, *96*(8), Article e11095. https://doi.org/10.1002/wer.11095
25. Xia, H., Pei, W., Huang, K., Shi, J., & Huan, G. (2025). Synergistic integration of vermicomposting and struvite crystallization for sustainable phosphorus recovery from sewage sludge: A low-carbon approach. *Waste Management*, *204*, Article 114926. https://doi.org/10.1016/j.wasman.2025.114926
26. Yan, X., Ding, J., Shi, W., Tang, L., Zhang, Y., & Xu, W. (2023). Synthesis of castor oil-based quaternary ammonium salt and modification of attapulgite for treating industrial wastewaters. *Materials*, *16*(9), Article 3468. https://doi.org/10.3390/ma16093468
27. Yang, J., Li, R., Zhou, Q., Li, L., Li, Y., Tu, C., Zhao, X., Xiong, K., Christie, P., & Luo, Y. (2021). Abundance and morphology of microplastics in an agricultural soil following long-term repeated application of pig manure. *Environmental Pollution*, *272*, Article 116028. https://doi.org/10.1016/j.envpol.2020.116028
28. Yang, K., Cheng, Z., Luo, W., Guo, B., Zhang, B., & Zhang, Y. (2023). Adsorption performance and mechanisms of MgO-modified palygorskite/biochar composite for aqueous Cd(II): Experiments and theoretical calculation. *Applied Surface Science*, *638*, Article 157965. https://doi.org/10.1016/j.apsusc.2023.157965
29. Yuan, T., Wang, J., Ren, Q., Zhao, B., Qin, J., Yan, W., & Wang, Z. (2025). Formation of iron-fluoride complexes compromises defluoridation efficiency of polymerized ferric sulfate: Performance

enhancement and mechanistic insights. *Journal of Environmental Chemical Engineering*, *13*(5), Article 117459. https://doi.org/10.1016/j.jece.2025.117459

30. Zhao, Y., Tai, J., Yao, S., & Li, S. (2023). High performance polymeric aluminum silicate sulfate (PASS) flocculant from abandoned molecular sieve. *Environmental Science and Pollution Research*, *30*(57), 119796–119803. https://doi.org/10.1007/s11356-023-30722-2
31. Zhu, Y., Wu, S., Liu, Z., Zheng, X., Zhao, M., Liu, S., Wang, L., & Fan, C. (2025). Optimization of flocculation-precipitation dewatering treatment for river sludge: Flocculant and conditioner dosage, organic matter content. *Journal of Environmental Chemical Engineering*, *13*(5), Article 118720. https://doi.org/10.1016/j.jece.2025.118720

Figures

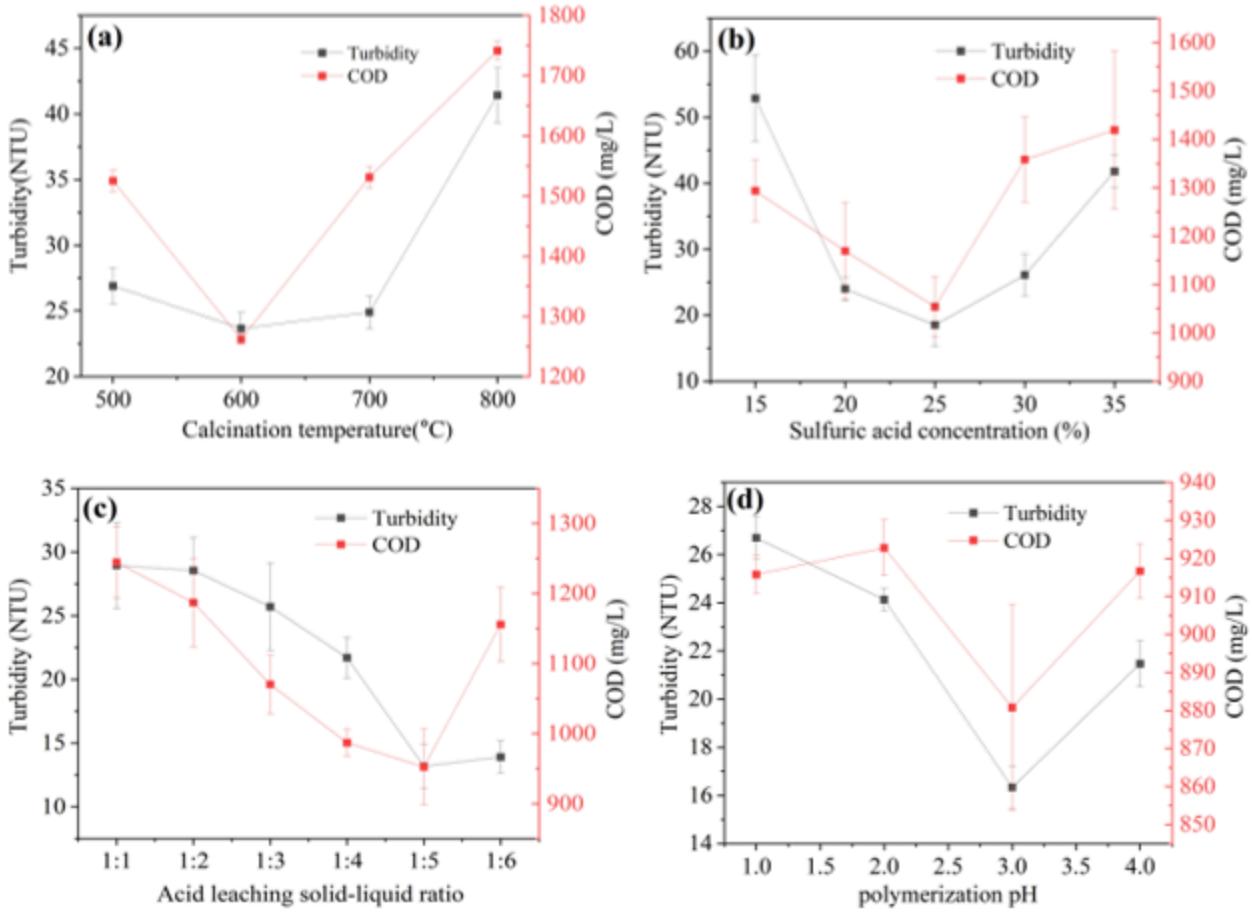


Figure 1

Effects of preparation parameters on the coagulation performance of ATPC. (a) calcination temperature; (b) sulfuric acid concentration; (c) acid leaching solid–liquid ratio; (d) polymerization pH.

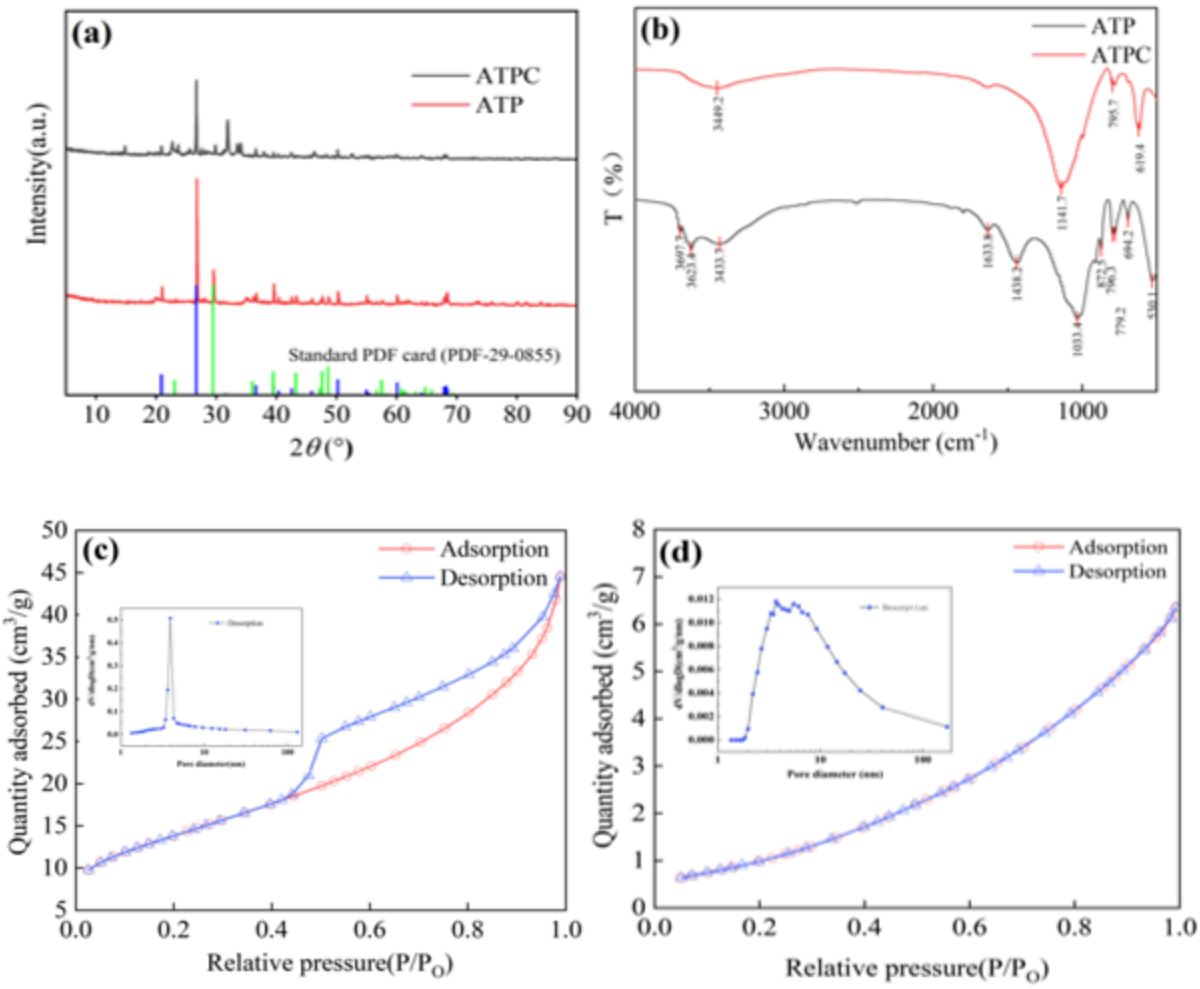


Figure 2

Structural characterization of raw ATP and modified ATPC. (a) XRD patterns; (b) FT-IR spectra; (c) N_2 adsorption–desorption isotherms of raw ATP; (d) N_2 adsorption–desorption isotherms of ATPC.

ATPC	1.63	2.98	26.54	4.30	55.10	6.26	0.84	0.54	1.82

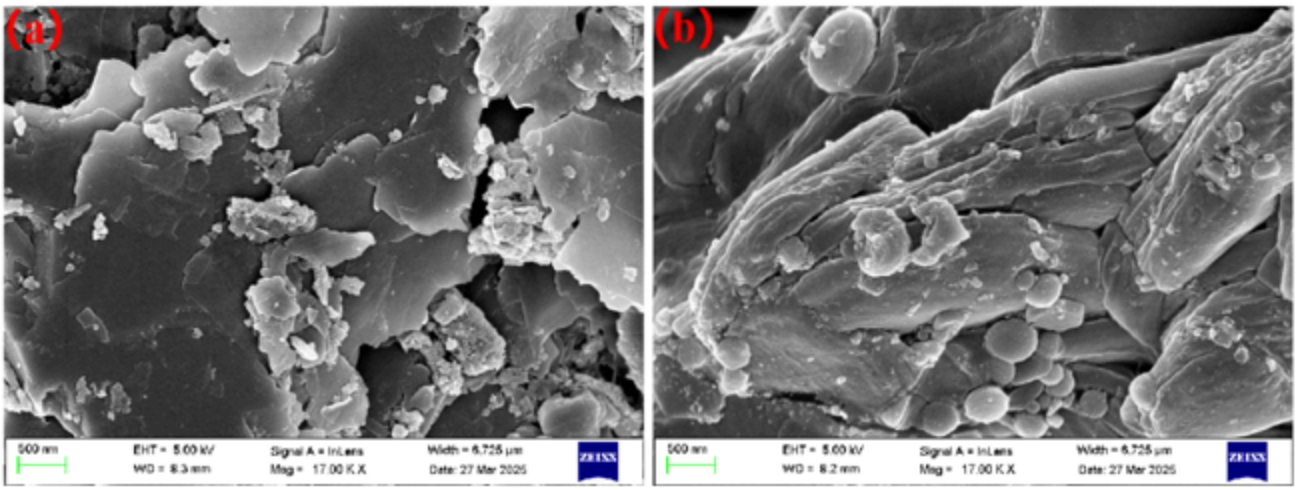


Figure 3

SEM images of (a) ATP and (b) ATPC.

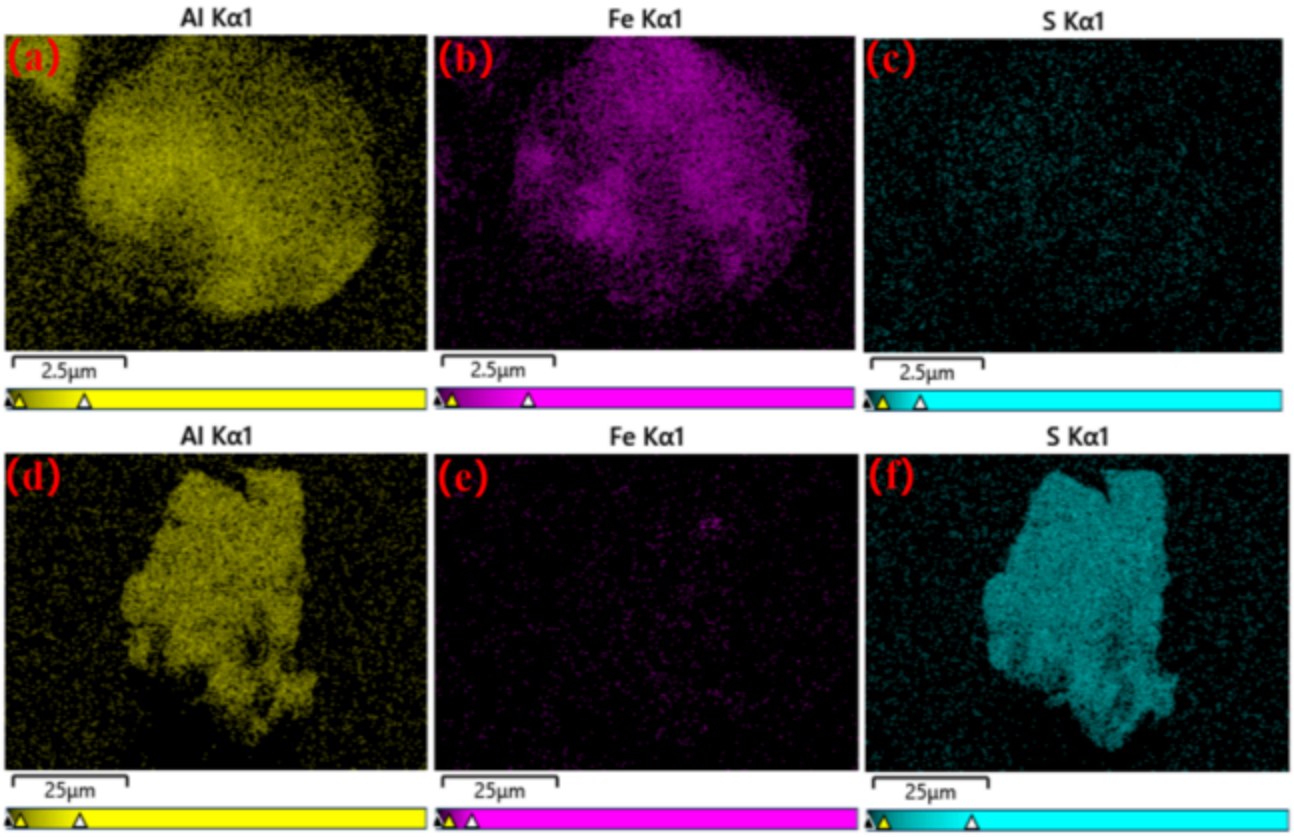


Figure 4

Elemental mapping images of (a) Al Kα1 in raw ATP; (b) Fe Kα1 in raw ATP; (c) S Kα1 in raw ATP; (d) Al Kα1 in ATPC; (e) Fe Kα1 in ATPC; (f) S Kα1 in ATPC.

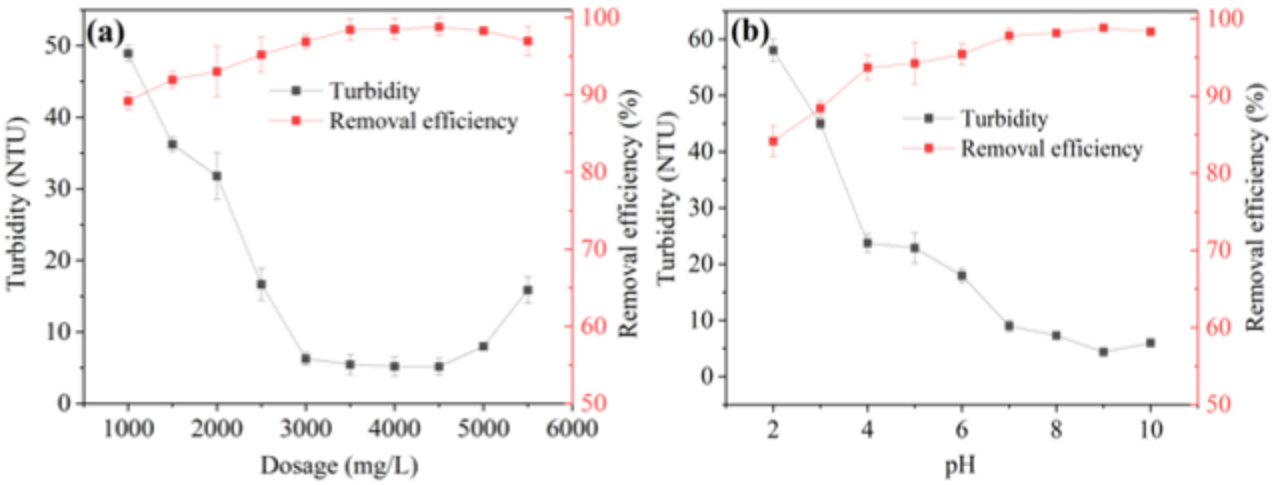


Figure 5

Effects of operational parameters on turbidity removal. (a) ATPC dosage; (b) initial pH.

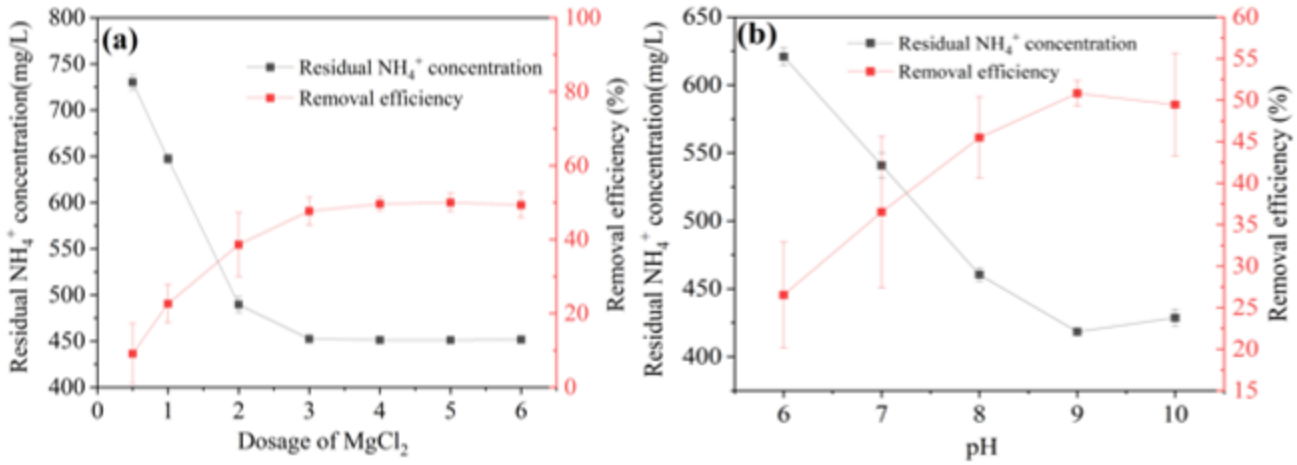


Figure 6

Effects of struvite crystallization parameters on NH_4^+–N removal. (a) $MgCl_2$ dosage; (b) initial pH.

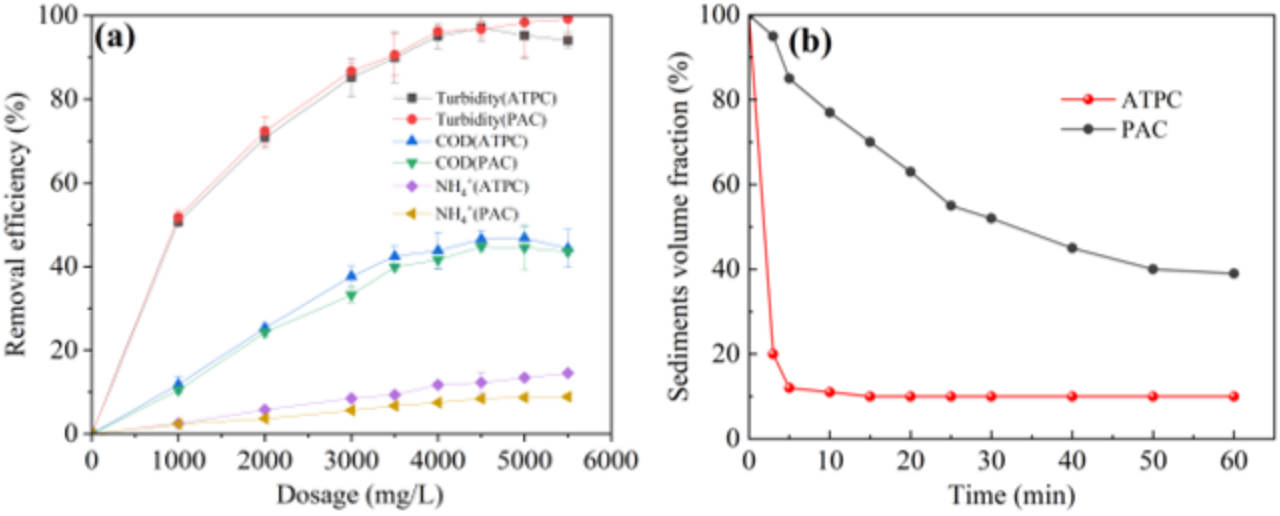


Figure 7

Coagulation performance comparison between ATPC and PAC. (a) Turbidity and NH_4^+ removal; (b) effect of settling time on the floc sedimentation volume.

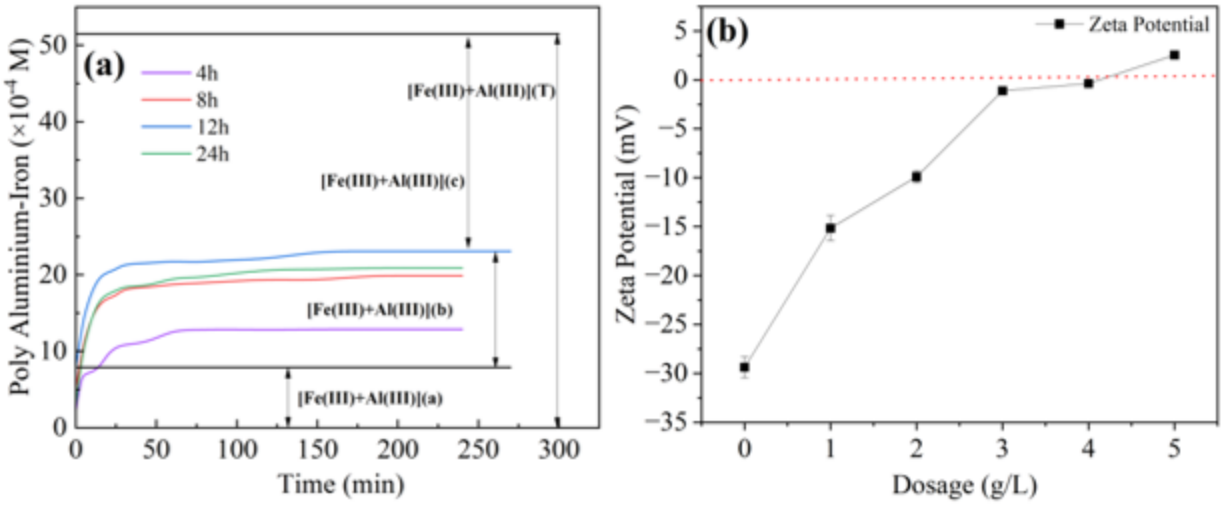


Figure 8

Aluminum–iron polymer speciation and zeta potential analysis. (a) Effect of aging time on the Al–Fe polymer distribution; (b) effect of ATPC dosage on the zeta potential.

Supplementary Files

This is a list of supplementary files associated with this preprint. Click to download.

- Originaldata.xlsx